京都大学防災研究所年報 第 53 号 B 平成 22 年 6 月
Annuals of Disas. Prev. Res. Inst., Kyoto Univ., No. 53 B, 2010

Morphological Changes induced by River Training Structures: Bandal-like structures and Groins

Hiroshi TERAGUCHI, Hajime NAKAGAWA, Kenji KAWAIKE, Yasuyuki BABA and Hao ZHANG

Synopsis

This paper is focused on the investigation of the characteristics of flow patterns and bed deformation around river training structures like groins with emphasis on the so-called bandal-like structures. Through laboratory experiments and numerical simulations, the complex sediment transport mechanism influenced by bandal-like structures is clarified. The experimental studies were conducted in a straight flume with two structures positioned on one side of channel for the measurements of the velocity field and deformed bed level near the structures under lived-bed scour condition. A morphological model based on unstructured meshes was developed to simulate the flow patterns and bed variation around the structures, which solves the RANS (Reynolds-averaged Navier Stokes) equations for 3D flow calculation with the standard k-ε model for turbulence closure, and the sediment transport calculation considering the bed load transport rate through the mass-balance equation. The experimental and numerical results for flow velocity distributions and deformed bed level around the structures field were analyzed and the applicability of bandal-like structures as a low cost alternative method compared to the conventional structures as groins is discussed.

Keywords: groins, bandal-like structure, unstructured meshes, non-submerged condition

1. Introduction

Nowadays, there are a variety of structures that can be called as river training structures as spur-dikes, groins, revetments, weirs, etc. Groins are usually used to create narrower and deeper river channel for navigation purposes, minimize bank erosion, and recently, restoring fish habitat to degraded streams and enhancing the diversity of the river ecosystem because diversified flow around groins creates conditions suitable for riverbank vegetation and aquatic biota (Carling et al, 1996; Schwartz and Kozerski, 2003). The flow field at a groin is coupled with a complex 3D separation of approach flow at upstream and periodic vortex shedding downstream of the structure. The complexity of flow increases with the development of the scour hole. The groin may be used in a channel to control the scour of riverbank and its development in the main channel direction. The scour estimation has attracted considerable research interest, and different prediction methods have been developed.

Most of the researchers have focused on scour at a conventional impermeable groin (or spur dike), such as Ahmad (1953), Garde et al. (1961), Gill (1972), Richardson and Stevens (1975), Rajaratnam and Nwachukwu (1983a), Shields et al. (1995), Kuhnle et al. (1999), Kothyari and Ranga Raju (2001) and Bharbhuiya and Dey (2004).

The researchers mainly focused on the local scouring depth and velocity distribution of a stable flow. Those two factors as well as the stability of structures are crucial parameters for its application.

Kwan (1989) and Kwan and Melville (1994) used hydrogen bubble technique to measure the 3D flow field in a scour hole at an abutment. It was observed that a primary vortex, which is similar to the horseshoe vortex at piers, associated with a downward flow being the main cause of scouring at abutments. Barbhuiya and Dey (2003) studies flow field in scour hole around abutments in straight channels. The 3D flow field at a vertical wall abutment was studied by Dey and Barbhuiya (2006). Studies of velocity profiles and scouring process in the vicinity of submerged dikes were performed by Elawady et al. (2000, 2001) and Nagy (2005), but more detailed investigation under submerged condition and considering different types of structures is also needed.

Review of literature shows that in spite of the importance of conventional structures as impermeable groins, less attention have been paid to study other types of structures as permeable groins (Mioduszewski et al., 2003) that can be used to minimize the occurrence of erosion around the structure due to the passage of flow through the structure and to reduce the flow velocity near the riverbank.

Other type of structure that was studied in details during this investigation due to the particular characteristics is the so-called bandal-like structure, i.e. local low cost structures commonly applied to improve or maintain the flow depths for navigation during low flow season in alluvial rivers of Indian Sub-Continent region like Bangladesh was studied. The essential characteristics of bandal-like structures are that there is an opening below (permeable part) to allow the passage of flow with reduced velocity through the structure and the sediment deposition near the riverbank, and the blockage of upper portion (impermeable part) to towards the near surface flow to the main channel direction.

Few studies including field investigations (Sharmin et al., 2007) and laboratory experiments were realized to verify the applicability of bandals in alluvial rivers. Rahman et al. (2004, 2006) verified the characteristics of flow patterns and sediment transport process around these structures in comparison with conventional impermeable groins under non-submerged condition. Furthermore it was studied the applicability of an analytical formula to predict the local scour around the structures including the erosion in the main channel. The basic features of bandals in terms of flow and sediment control were clarified under clear-water scour condition. However, investigations with different bandal spacing and alignment, experiments under lived-bed scour condition, and also the effect of submergence during flood events is required to obtain the detailed information about the applicability of the bandals.

To better understand the mechanisms by which the bandal-like structure affect the flow dynamics and river channel morphology, an assessment of river training structures was accomplished by laboratory experiments and numerical model simulations. The experiments were conducted in a straight flume with movable bed to study the influence of two hydraulic structures on the flow field and bed deformation under non-submerged condition. It was used impermeable and permeable groins and the bandal-like structures. These results, when interpreted in conjunction with numerical and field studies, can provide important information for the advanced, environmentally oriented design of bandal-like structures.

2. Laboratory experiments

2.1 Experimental set-up

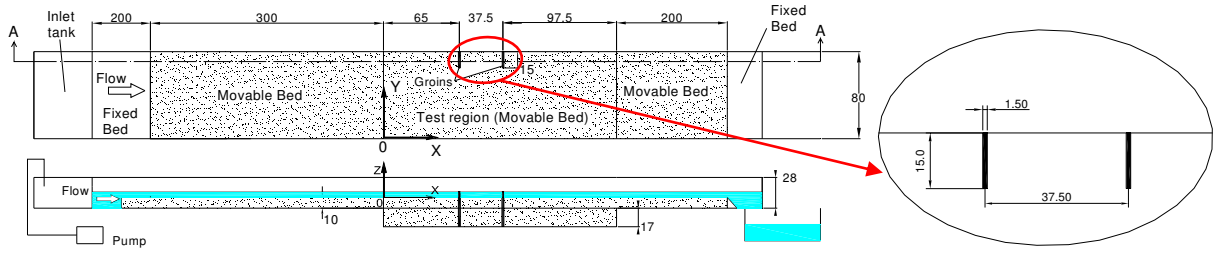

Fig.1 Experimental setup (plan-view: top; section A-A: bottom; right side: detail of structures) (Unit:cm)

The experimental studies were carried out at Ujigawa Open Laboratory, DPRI, Kyoto University, in a straight flume with 10m-long, 0.80m-wide and 0.28m-deep (0.45m-deep in the test region). The detailed sketch of the experimental set-up is shown in Fig.1. The channel slope was adjusted to be 1/800. The structures having a streamwise length (L) of 0.015m was embedded in a coal (powdered anthracite) recess with 8.50m long, 0.80m wide and 0.10m deep (0.27m deep in the test region), which retained coal (d_{50}=0.835mm and ρ_s=1410kg/m^3). The groins were attached to the steel-wall of the flume according to the Fig.1. The coal recess was located 2.0m downstream of the flume inlet. A false floor at an elevation of 0.10m from the flume bottom and 1.0m long was fixed at the upstream before the movable part to reduce the water surface variation. A calibrated V-notch weir, fitted at the inlet of the flume, was used to measure the inflow discharge. The water depth in the flume was adjusted by a steel tailgate located at the downstream end. A vernier point gauge with an accuracy of ±0.5 mm was used to measure the water levels.

2.2 Experimental procedure

The hydraulic conditions adopted for the experiments are given in Table 1. Before starting each experimental run, the flume was slowly filled up with water by a plastic pipe from the downstream end. Once the required water depth was reached and the correct discharge was adjusted, the experiment was run under live-bed scour condition. The approach flow depth (h) varies depending on the studied case. The Shields diagram was used to determine the critical shear velocity u_{*c} for the sediment (coal) material.

The experiment was run for a period of 6 hours that is the required time to achieve the dynamic equilibrium condition accordingly to the previous tests. Then, the flow discharge was reduced gradually to prevent any undesirable movement of the bed material. In order to determine the final bed deformation contour, the remaining water was carefully draining out from the flume and the scour depths at different cross-sections were measured using a laser displacement sensor (Model: LK-2500). After the deformed bed level measurements, an instant cement powder was spread uniformly over the scoured bed to fix it. The sediment sufficiently impregnated with the cement powder was left to dry for a period of 24 h.

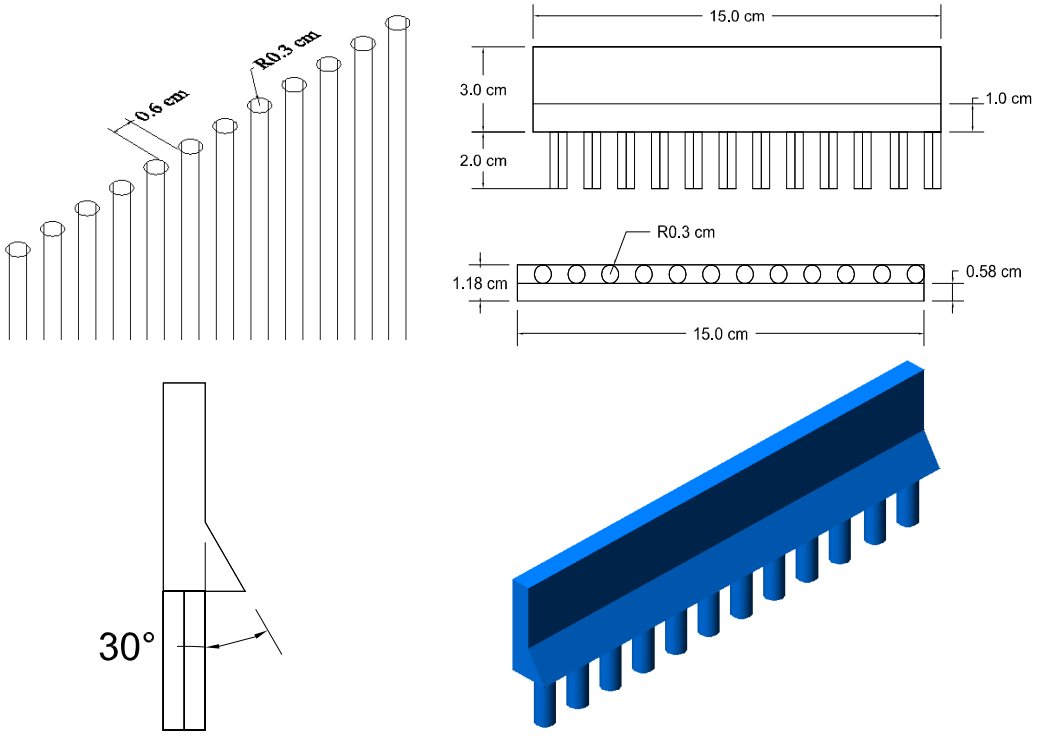

Fig.2 Details of permeable groin (top-left side) and bandal-like structure (geometry:top-right and bottom-left sides; isometric view:bottom-right side)

Having dried further up to 24h, the scoured bed profile became rock hard, facilitating the flow velocity measurements. The complex three-dimensional velocity components were measured by electromagnetic current meters (Model: ACM250-A, Alec Electronics Co., LTD). The current meter comprised one probe with I-shape to measure the velocity in horizontal direction (plane X-Y) and another probe with L-shape to measure the velocity in the vertical direction (planes X-Z or Y-Z), connected to an analogical/digital signal converter. The probe (I or L shapes) are positioned into the water and fixed by a Vernier point gauge to determine the velocity on the desired position and then connected to a notebook through a data logger card to store the measured data. The water surface velocity measurements was realized using the PIV technique (Fujita et al., 1998) through the acquisition of flow pattern images using a video camera and PVC powder as a tracer.

The X-axis starts from the beginning of the test region (movable bed), the Y-axis from the right side wall of the flume and the Z-axis from the initial flat bed level. The impermeable groins were made of wooden cuboids with 1.5cm thickness, while the permeable groins were made with a series of steel round sticks with a diameter equal to 0.6cm-each and designed to have a permeability of 50%. The bandal-like structures are made using the permeable groins configuration and blocking the upper half part with a steel plate to represent the bended plate (see Fig. 2).

Table 1 – Details of experimental conditions

Type of groin*	I	P	BS
Cases	1	2	3
Submergence	Non-submerged		
Discharge Q(l/s)	7.76		
Mean velocity u(cm/s)	24.25		
Flow depth h(cm)	4.00		
Shear velocity u_*(cm/s)	2.22		
Shear velocity ratio u_*/u_{*c}	1.91		
u_*/w_s	0.573		
Reynolds number, Re	7,406		
Froude number, Fr	0.387		

*I–impermeable groin; P–permeable groin; BS–bandal-like structure

3. Numerical modeling

3.1. Hydrodynamic Model

The governing equations for the flow calculations are based on the 3D RANS (Reynolds-averaged Navier-Stokes equations) and the continuity equation, which can be expressed in a Cartesian coordinate system with the tensor notation as follows.

$$\frac{\partial u_i}{\partial t} + u_j \frac{\partial u_i}{\partial u_j} = F_i - \frac{1}{\rho}\frac{\partial p}{\partial x_i} + \nu \frac{\partial^2 u_i}{\partial x_j \partial x_j} + \frac{1}{\rho}\frac{\partial \tau_{ij}}{\partial x_i} \quad (1)$$

$$\frac{\partial u_i}{\partial x_i} = 0 \quad (2)$$

where u_i=time-averaged velocity components (i = 1, 2, 3); x_i=Cartesian coordinate component; ρ =density of the fluid; F_i=body force; p=time-averaged pressure; ν=molecular kinematic viscosity of the fluid; $\tau_{ij} = -\rho\overline{u_i' u_j'}$, are the Reynolds stress tensors, and u_i' is the fluctuating velocity component. The k-ε model is used for the turbulence closure. The Reynolds tensors are acquired through the linear constitutive equation.

$$-\overline{u_i' u_j'} = 2\nu_t S_{ij} - \frac{2}{3}k\delta_{ij} \quad (3)$$

where k=turbulence kinetic energy; δ_{ij}=the Kronecker delta; ν_t= eddy viscosity and S_{ij}=the strain-rate tensor and ε is the dissipation rate of the turbulence kinetic energy k. The model constants are used as suggested by Rodi (1980). A detailed presentation about the numerical schemes, discretization methods, solution methods, equation solvers and the convergence criteria is given by Zhang et al. (2006). In the simulation, the inlet boundary is considered as a Dirichlet boundary and all the quantities are prescribed. The outlet boundary has been set far from the groin area, a Neumann boundary with zero gradients is assumed there. The wall function approach is adopted near impermeable boundaries and each pile (permeable groin) and bandals (upper bended plate and lower permeable opening) is expressed with some fine meshes in the simulation. The simulation sequence follows the SIMPLE (Semi-Implicit Method for Pressure-Linked Equations) procedure.

3.2. Sediment Transport Model

The sediment transport in open-channels is

governed by the sediment mass-balance equation integrated over the water depth h, described below.

$$(1-\lambda)\frac{\partial z_b}{\partial t}+\frac{\partial(q_{Tx})}{\partial x}+\frac{\partial(q_{Ty})}{\partial y}+(E-D)=0 \quad (4)$$

where z_b=local bed level above datum; λ=porosity of the bed material and q_{Tx}, q_{Ty} =components of the total-load sediment transport in the x and y directions, respectively, E=the upward near-bed flux and D=the downward near-bed flux. For calculating the sediment transport rate, it is subdivided into bed load and suspended load.

1) Bed load transport

The bed load transport is calculated by using the Ashida-Michiue's empirical formula.

$$\frac{q_b}{\sqrt{(s-1)gd^3}}=17\tau_{*e}^{\frac{3}{2}}\left(1-\frac{u_{*c}}{u_*}\right)\left(1-\frac{\tau_{*c}}{\tau_*}\right) \quad (5)$$

where q_b=bed load; s=specific gravity of sediment; d=diameter of sediment; τ_*, τ_{*c}, τ_{*e}=dimensionless shear stress, critical shear stress and effective shear stress, respectively; u_*, u_{*c}=friction velocity and critical friction velocity, respectively. In the bandals simulations, the deformed bed from the experimental results was used as a fixed bed during the flow calculations.

4. Results and Discussions

4.1 Velocity distributions

1) Velocity distribution around the structures in X-Y plane at water surface (horizontal plane)

The measured and calculated flow velocity distributions results around the different types of structures in horizontal plane are shown in Figs. 3, 4, and 5. When the flow approaches the upstream groin in Case 1 (Figs. 3a and 3b) the obstructed flow towards to the main channel creating a mixing zone in front of the groin head. This flow travels to downstream which creates recirculation flow in between region of groins and also at downstream of groins near the riverbank. Comparing the measured and simulated results, the flow structures are quite similar around the structures. Due to the refinement of mesh used in the calculations, the recirculation flow is clearly observed between the two groins and also the flow separation at upstream groin head.

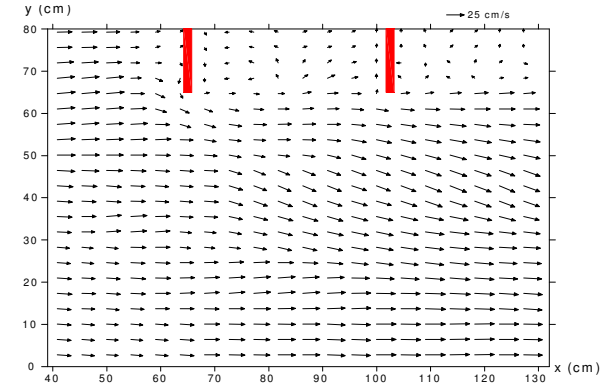

Fig.3a Flow velocity (u,v) on water surface by PIV in Case 1 – Impermeable groins (Experiment)

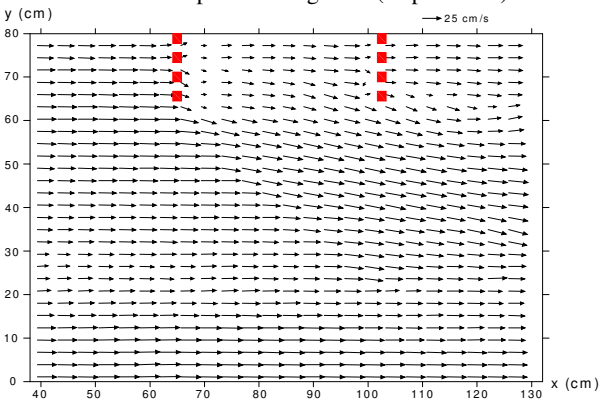

Fig.3b Flow velocity (u,v) on water surface in Case 1 – Impermeable groins (Simulation)

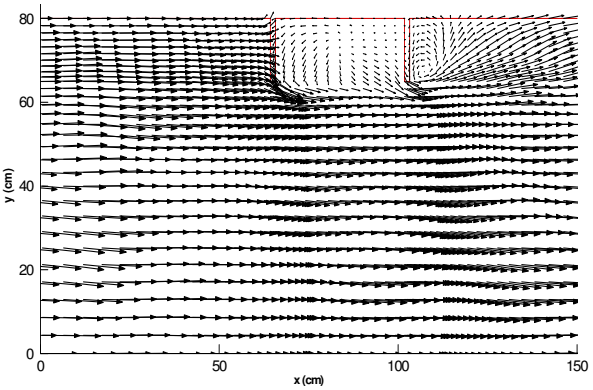

Fig.4a Flow velocity (u,v) on water surface by PIV in Case 2 – Permeable groins (Experiment)

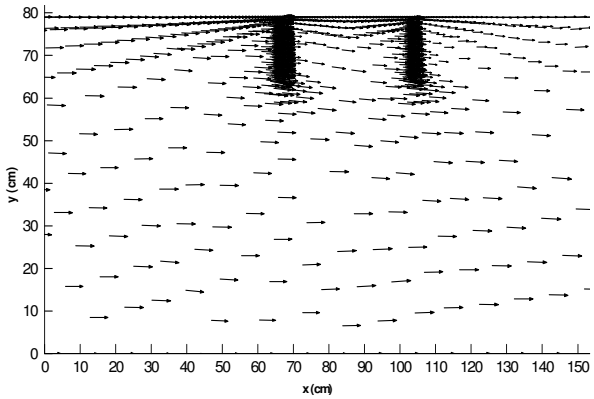

Fig.4b Flow velocity (u,v) on water surface in Case 2 – Permeable groins (Simulation)

The permeable groins (Figs. 4a and 4b) show that the flow direction is not greatly changed resulting practically parallel to the channel direction. It is quite different compared to the impermeable groins case. The flow direction towards to the main channel at groins head in both experimental and simulation results, however with small intensity due to the groins permeability. At the downstream of the upstream groin, reduction of velocity occurs near the bank and after the flow passing the downstream groin the reduction becomes more significant. This reduction is important to the riverbank protection and can contribute to the sediment deposition near the groins field.

Observing the case of bandal-like structures, it is possible to observe differences of flow patterns especially in the area between the two structures due to the passage of flow through the lower opening of bandal. In Figs. 5a and 5b, it can be seen that the flow after passing the upstream structure towards to the main channel direction, which prevents the formation of recirculation currents over there. Also a reduction of velocity magnitude occurs due to the flow separation caused by the upper half bended plate that deviate the near surface flow to the main channel direction.

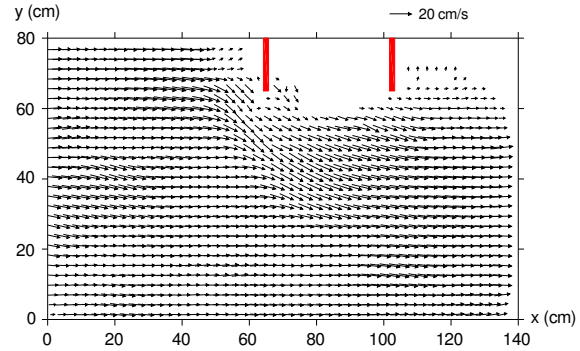

Fig.5a Flow velocity (u,v) on water surface by PIV in Case 3 – Bandal-like structures (Experiment)

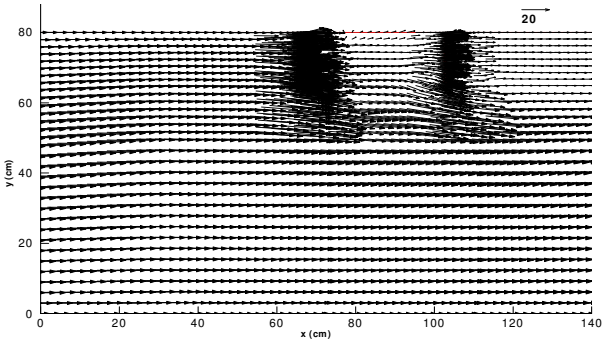

Fig.5b Flow velocity (u,v) on water surface by PIV in Case 3 – Bandal-like structures (Simulation)

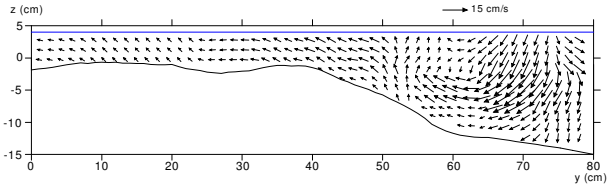

Fig.6a Flow velocity (v,w) at x=62.0cm in Case 1 – Impermeable groins (Experiment)

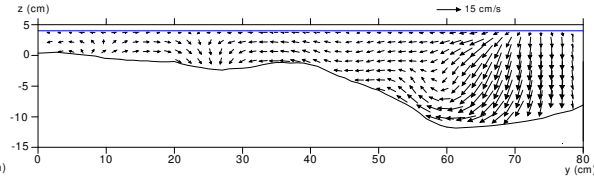

Fig.6b Flow velocity (v,w) at x=62.0cm in Case 1 – Impermeable groins (Simulation)

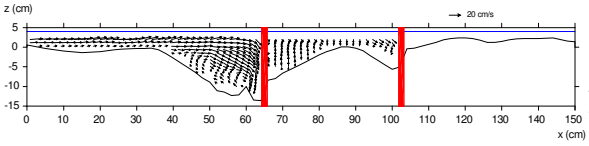

Fig.7a Flow velocity (u,w) at y=72.0cm in Case 1 – Impermeable groins (Experiment)

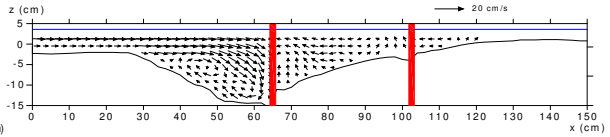

Fig.7b Flow velocity (u,w) at y=72.0cm in Case 1 – Impermeable groins (Simulation)

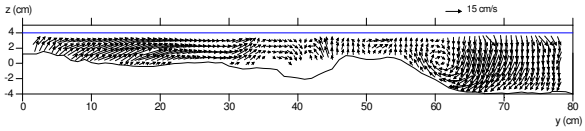

Fig.8a Flow velocity (v,w) at x=62.0cm in Case 3 – Bandal-like structures (Experiment)

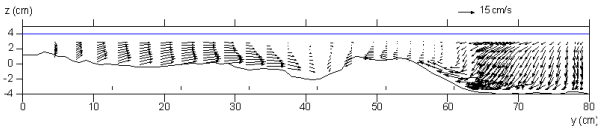

Fig.8b Flow velocity (v,w) at x=62.0cm in Case 3 – Bandal-like structures (Simulation)

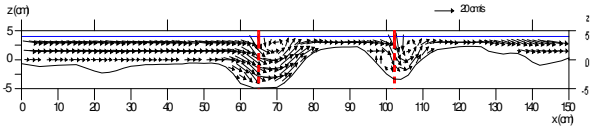

Fig.9a Flow velocity (u,w) at y=72.0cm in Case 3 – Bandal-like structures (Experiment)

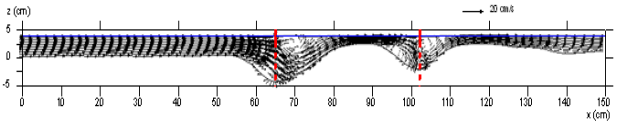

Fig.9b Flow velocity (u,w) at y=72.0cm in Case 3 – Bandal-like structures (Simulation)

2) Velocity distribution at sections in Y-Z and X-Z planes (vertical direction)

More detailed insight into the complex 3D flow velocity distribution around the structures can be obtained by analyzing the velocity profiles at the cross-section (Y-Z plane) and longitudinal-section (X-Z plane) showed in Figs. 6, 7, 8, and 9. The comparison was made between the bandal-like structures and the impermeable groins cases (Cases 1 and 3) due to the facility to distinguish the influence of these structures on flow patterns**.** The described sections are positioned at x=62.0cm (cross-section), just 2.25cm upstream of the upstream structure (looking from downstream to upstream) and y=72.0cm (longitudinal-section) in the middle part of the structures (length=15.0cm).

Verifying the experimental results, the vertical vortices formed near the upstream structure caused by the downward flow is quite similar to the computed results in both cases. However, the bandal case shows higher flow velocity near the surface deviated to the main channel which is more effective than the impermeable groins case due to the effect of upper bended plate which directs the near surface flow to the main channel minimizing the effect on the bed near the structure. This point is an important characteristic of bandal that will be discussed in details during the analysis of bed deformation results. The longitudinal-section shows clearly the downward flow at upstream of both bandals that induces the formation of vortices at upstream of structure. At the downstream of each structure, the flow passing through the lower permeable part with reduced velocity show similar vertical vortex with small magnitude that can increase the deposition process over there.

4.2 Bed deformation

The comparisons between the experimental and simulated results of bed level contours at equilibrium condition in Cases 1 and 2 are shown in Figs.10 and 11. In the bandals case (Case 3), only the experimental result is showed in Fig.12.

The mostly used impermeable groins (Case 1) showed the similar results studied by Rajaratnam and Nwachukwu (1983a; 1983b) and Melville (1992) with a huge erosion at upstream of groin, in this case the upstream one, when compared to the permeable groins and bandal-like structures (Cases 2 and 3). The previously described formation of downward flux due to the blockage of flow in Case 1 is the main reason for the deepest erosion at the upstream region and it's possible to verify this characteristic in the simulated results (Fig. 10b).

In Case 3 with bandals, the upper bended plate towards the near surface flow with high velocities to the main channel direction and the flow passing through the lower part (piles) minimize the effects of the downward flux, and the same effect is observed in the permeable groins (Case 2), where the resulted erosion is very small than the other cases in both experiment and simulation (Figs. 11a and 11b) due to the small reduction of flow velocity compared to the bandal-like structure case.

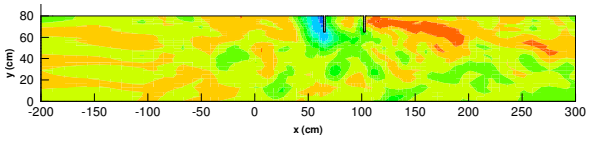

Fig.10a Bed level contour in Case 1 – Impermeable groins (Experiment)

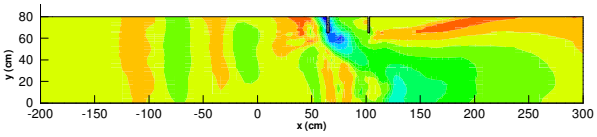

Fig.10b Bed level contour in Case 1 – Impermeable groins (Simulation)

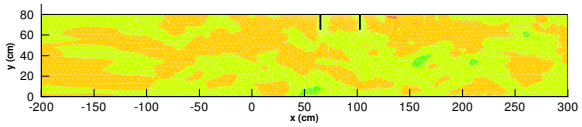

Fig.11a Bed level contour in Case 2 – Permeable groins (Experiment)

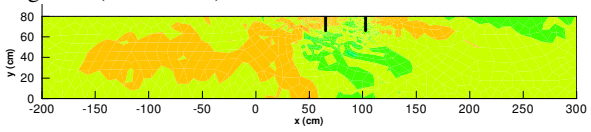

Fig.11b Bed level contour in Case 2 – Permeable groins (Simulation)

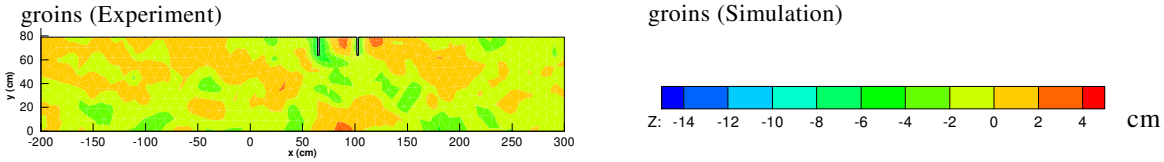

Fig.12 Bed level contour in Case 3 – Bandal-like structures (Experiment)

The flow separation that can be seen very clearly in Case 1 (Fig. 4a) is responsible for the formation of recirculation currents in the region between the groins causing the erosion near the riverbank observed in Figs 10a and 10b. At downstream of groins, the return currents with low velocities formed near the bank side cause the deposition of sediment that is clearly verified in Fig. 10.

Similar flow separation occurs in the bandal-like structures (Figs. 5a and 5b), however due to the effect of upper bended plate at upstream and the flow passing through the lower permeable area at downstream of structure, the recirculation currents can't be formed reducing the probability of erosion near the bank. Therefore, this structure can be used as a riverbank protection.

The deposition process around the bandal-like structure shows promising results compared to the other structures in between and at downstream of the structures field. The reduction of flow velocity passing through the lower opening (piles) in both structures (Fig.9) contributes to the deposition of sediment carried by the flow at the downstream of structure and near the riverbank. On the other hand, in Case 2 (permeable groins) the same phenomenon can be observed, however the deposited volume of sediment is very different because only a little reduction of flow velocity occurs and the sediment transported by the flow is carried to the downstream of channel. In this case the deposition area is distributed throughout the channel with a small concentration at downstream of groins.

5. Conclusions

This study provided us detailed information regarding to the flow patterns and bed deformation around bandal-like structures under lived-bed scour and non-submerged conditions. Under the same hydraulic conditions, the conventional structures like impermeable and permeable groins were investigated to verify the similarities and the differences between them and the bandal-like structures, considering the flow velocity distributions and bed deformation around the structures. The analysis of these results clarified the mechanism of sediment transport process influenced by the presence of bandal-like structures and showed us promising results when compared with the other two types of structures, i.e. the small erosion around the structures and the deposition especially near the bank can serve to protect the riverbank from erosion, and a strong tendency to erode the main channel can be useful to the formation of deeper channel for navigation purposes in rivers.

The numerical model results show a reasonable agreement analyzing the flow patterns in all cases, especially the flow around the complex structures as permeable groins and bandal-like structures. The sediment transport calculations showed satisfactory estimation of bed deformation considering only bed load transport, however the occurrence of suspended sediment near the structures observed during the experiments need to be investigated with the inclusion of suspended sediment calculation in the sediment transport model. Also, movable bed simulations of bandal-like structures are expected to be done in the next step to validate the numerical model proposed. Simulations under submerged conditions are expected to be done with the same structures in the future investigations.

References

Ahmad, M. (1953): Experiments on design and behavior of spur dikes, Proceeding of International Hydraulic Convention, ASCE, New York, pp. 145-159.

Ashida, K. and Michiue, M. (1972): Studies on bed load transportation for nonuniform sediment and river bed variation, Disaster Prevention Research Institute Annuals, Kyoto University, No. 14B, pp. 259-273 (in Japanese).

Barbhuiya, A. K., and Dey, S. (2003): Vortex flow field in a scour hole around abutments, International Journal of Sediment Research, Vol. 18, No. 4, pp. 310-325.

Barbhuiya, A. K., and Dey, S. (2004): Local scour at abutments: A Review, Sadhana, Vol. 29, Part. 5, pp. 449-476.

Carling, P.A., Kohmann, F., and Golz, E. (1996): River hydraulics, sediment transport and training works: their ecological relevance to European rivers, Archiv. Hydrobiol. Suppl., Vol. 113, No. 10, pp 129-146.

Demuren, A. O., and Rodi, W. (1986): Calculation of flow and pollutant dispersion in meandering channels, Journal of Fluid Mechanics, Cambridge, U.K, Vol. 172, pp. 63-92.

Demuren, A. O. (1989): Calculation of sediment transport in meandering channels, Technical Session A, Proc. 23rd IAHR Congress, International Association for Hydraulic Research, Delft, The Netherlands.

Dey, S., and Barbhuiya, A. K. (2006): Velocity and turbulence in a scour hole at a vertical-wall abutment, Flow Measurements and Instrumentation, Vol. 17, pp. 13-21.

Einstein, H. A. (1950): The Bed-Load Function for Sediment Transportation in Open Channel Flows, Technical Bulletin No. 1026, United States Department of Agriculture.

Elawady, E., Michiue, M., and Hinokidani, O. (2000): Experimental Study of Flow Behavior around Submerged Spur-dike on Rigid Bed, Annual Journal of Hydraulic Engineering, JSCE, Vol. 44, pp. 539-544.

Elawady, E., Michiue, M., and Hinokidani, O. (2001): Movable Bed Scour around Submerged Spur-Dikes, Annual Journal of Hydraulic Engineering, JSCE, Vol. 45, pp. 373-378.

Fujita, I., Muste, M., and Kruger, A. (1998): Large scale particle image velocimetry fro flow analysis in hydraulic engineering applications, Journal of Hydraulic Research, vol. 36, No. 3, pp. 397-414.

Garde, R. J., Subramanya, K. and Nambudripad, K. D. (1961): Study of scour around spur-dikes, Journal of Hydraulic Division, ASCE, Vol. 87, No. 6, pp. 23-38.

Gill, M.A. (1972): Erosion of sands beds around spur dikes, Journal of Hydraulic Division, ASCE, Vol. 98, No. 9, pp. 1587-1602.

Ishigaki, T., and Baba, Y. (2004): Local scour induced by 3D flow around attracting & deflecting groins, Proc. 2nd Int. Conf. on Scour and Erosion, Meritus Mandarim, Singapore, pp. 301-308.

Itakura, T., and Kishi, T. (1980): Open Channel Flow with Suspended Sediments, Journal of Hydraulic Division, ASCE, Vol.106, No. 8, pp. 1325-1343.

Klaassen, G. J., Douben, K. and van der Waal, M. (2002): Novel approaches in river engineering, River flow 2002, Bousmar & Zech, eds., Swets & Zeitlinger, Lisse, pp. 27-42.

Kothyari, U. C., and Ranga Raju, K. J. (2001): Scour around spur dikes and bridge abutments, Journal of Hydraulic Research, Vol. 39, No. 4, pp. 367-374.

Kuhnle, R. A., Alonso, C. V., and Shields, F. D. (1999): Geometry of scour holes associated with 90o spur dikes, Journal of Hydraulic Engineering, ASCE, Vol. 125, No. 9, pp. 972-978.

Kuhnle et al. (2002): Local scour associated with angled spur dikes, ASCE, Journal of Hydraulic Engineering, Vol. 128, No. 12.

Kwan, T. F. (1989): A study of abutment scour, Report No. 451, School of Engineering, University of Auckland, Auckland, New Zealand.

Kwan, T. F., and Melville, B. W. (1994): Local scour and flow measurements at bridge abutments, Journal of Hydraulic Research, Vol. 32, No. 5, pp. 661-673.

Melville, B.W. (1992): Local scour at bridge abutments, Journal of Hydraulic Engineering, ASCE, Vol. 118, No. 4, pp. 615-630.

Melville, B. W., and Coleman, S. E. (2000): Bridge Scour, Water Resources Publications, Highlands Ranch, Colorado.

Mioduszewski, T., Maeno, S., and Uema, Y. (2003): Influence of the Spur Dike Permeability on Flow and Scouring during a Surge Pass, International Conference on Estuaries and Coasts, Hangzhou, China, pp. 380-388.

Nagata, N., Hosoda, T., Nakato, T., and Muramoto, Y. (2005): Three-dimensional numerical model for flow and bed deformation around river hydraulics structures, Journal of Hydraulic Engineering, ASCE, Vol. 131, No. 12, pp. 1074-1087.

Nagy, H. M. (2005): Hydraulic evaluation of emerged and submerged spur-dikes: temporal bed evolution and equilibrium state characteristics, Alexandria Engineering Journal, Vol. 44, No. 2, pp. 279-290.

Onda, S., Hosoda, T., Kimura, I., and Iwata, M. (2007): Numerical simulation on local scouring around a spur dyke using equilibrium and non-equilibrium sediment transport models, Annual Journal of Hydraulic Engineering, JSCE, Vol. 51, pp. 943-948.

Peng, J., Tamai, N., Kawahara, Y., and Huang, G. (1999): Numerical modeling of local scour around

spur dikes, Proceedings of 28th IAHR Congress, Graz, Austria.

Rahman, M. M., Nakagawa, H., Khaleduzzaman, A. T. M., Ishigaki, T., and Muto, Y. (2004): On the formation of stable river course, Annuals of Disaster Prevention Research Institute, Kyoto University, No. 47B, pp. 601-616.

Rahman, M. M., Nakagawa, H., Ito, N., Haque, A., Islam, T., Rahman, M. R., and Hoque, M. M. (2006): Prediction of Local Scour Depth around Bandal-like Structures, Annual Journal of Hydraulic Engineering, JSCE, Vol. 50, pp. 163-168.

Rajaratnam, N, and Nwachukwu, B. A. (1983a): Erosion near groyne structures, Journal of Hydraulic Research, IAHR, Vol. 21, No. 4, pp. 227-287.

Rajaratnam, N, and Nwachukwu, B. A. (1983b): Flow near groyne-like structures, Journal of Hydraulic Engineering, ASCE, Vol. 109, No. 3, pp. 463-480.

Richardson, E. V., and Stevens, M. A. (1975): The Design of Spurs for River Training, Proceeding of the 15th Congress of the International Association for Hydraulic Research, IAHR, Basil, Vol. 2, pp. 382-388.

Rodi, W. (1980): Turbulence models and their application in hydraulics – a state of art review, University of Karlsruhe, Germany.

Schwartz, R. and Kozerski, H. (2003): Entry and deposits of suspended particulate matter in groyne fields of the middle Elbe and its ecological relevance, Acta Hydrochim. Hydrobiol., Vol. 31, No. 4-5, pp 391-399.

Sharmin, R., Rahman, M. M., Martin, A., Haque, E., Hossain, I., and Razzak, A. (2007): Effectiveness of Bandalling and dredging for the maintenance of navigation channel in the Jamuna River, Int. Conf. on Water & Flood Management, March 12-14, Dhaka, Bangladesh, pp. 125-133.

Shields, F. D., Cooper, C. M., and Knight, S. S. (1995): Experiments in stream restoration, Journal of Hydraulic Engineering, Vol. 121, No. 6, pp. 494-502.

Shields, F. D., Jr., Copeland, R. R., Klingeman, P. C., Doyle, M. W., and Simon, A. (2003): Design for stream restoration, Journal of Hydraulic Engineering, Vol. 129, No. 8, pp. 575-584.

Surian, N., and Rinaldi, M., 2003, Morphological response to river engineering and management in alluvial channels in Italy, Geomorphology, Vol. 50, No. 4, pp. 307-326.

Tominaga, A., and Matsumoto, D. (2006): Diverse riverbed figuration by using skew spur-dike groups, River flow 2006, Lisbon, pp. 683-691.

Uijttewaal, W. S. J. (2005): Effects of groin layout on the flow in groin fields: laboratory experimental, Journal Hydraulic Engineering, ASCE, Vol. 131, No. 9, pp. 782-791.

Van Rijn, L. C. (1987): Mathematical modeling of morphological processes in the case of suspended sediment transport, Delft Hydr. Communication, No. 382.

Wang, S. S. Y., and Adeff, S. E. (1986): Three-dimensional modelling of river sedimentation processes, Proc., 3rd International Symposium on River Sedimentation, University of Mississippi, Missouri.

Wu, W., Rodi, W., and Wenka, T. (2000): 3D numerical modeling of flow and sediment transport in open channels, Journal of Hydraulic Engineering, Vol. 126, No. 1, pp. 4-15.

Zhang, H. (2005): Study on Flow and Bed Evolution in Channels with Spur Dykes, Doctoral Dissertation, Kyoto University.

Zhang, H., Nakagawa, H., Muto, Y., Baba, Y. and Ishigaki, T. (2006): Numerical simulation of flow and local scour around hydraulic structures, River flow 2006, pp. 1683-1693.

バンダル及び水制による河床形態への影響

Hiroshi TERAGUCHI・中川一・川池健司・馬場康之・張浩

要　旨

本論文ではバンダル水制がもたらす流れおよび河床形成について着目し，移動床実験と数値解析によってバンダル水制周辺の複雑な流砂メカニズムを明らかにした。移動床実験では片側に２基の水制を設置した直線水路を用い，流れおよび局所洗掘された水制周辺の河床高計測をおこなった。数値計算で用いた河床変動モデルは非構造格子を用いており，流れは３次元のRANS(Reynolds-averaged Navier Stokes)方程式と標準k-εモデルを解き，掃流砂の連続方程式により河床高変化を計算している。水制周辺の河床形状と流速分布の実験および計算結果を解析し，従来の水制構造物に比べて安価なバンダル水制の適用性について考察を行った。

キーワード: 水制，バンダル，非構造格子，非越流